

Residual Strengths of Reinforced Concrete Beams With Heavy Deterioration

¹Wei-lun Wang and ²Ju Chen

¹College of Civil Engineering, Shenzhen University, China

²Department of Civil Engineering, Zhejiang University, Hangzhou 310027, P.R. China

Abstract: This study focused on the residual strengths of reinforced concrete beams with heavy deterioration. This work is based on experimental investigation of reinforced concrete beams naturally corroded over 30 years. Visual inspection was firstly conducted and the concrete cracking, spalling of concrete cover, corrosion of rebar were recorded. Material tests on concrete and corroded rebar were also conducted. Loading tests were performed on three corroded beams. The residual bending strengths obtained from the test results were compared with design strengths of uncorroded beam. It is shown that the corroded beams lost most of their strengths. Finite element model was developed to further investigate the behaviour of corroded reinforced concrete beams. The element type and mesh, boundary condition and load application, and material model were considered in the nonlinear finite element model. The effect of concrete cover spalling, rebar corrosion and mid-span vertical crack on the residual strength of corroded reinforced concrete beams were analyzed using the developed model.

Key words: Design, deterioration, finite element model, reinforced concrete beams

INTRODUCTION

Premature deterioration caused by reinforcement corrosion is being reported in an increasing number of structures. In general, corrosion is caused by the destructive attack of chloride ions incorporation into the concrete mixture, by carbonation of the concrete cover, or their combination (Andrs *et al.*, 2007). The estimated corrosion damage of bridge deck and support structures in the USA alone ranges between \$170 and \$550 million and replacement cost of RC structures could be substantially higher (Pandey and Banerjee, 1998). In addition to the economical losses incurred, public safety is also affected. Losses of life associated with the collapse of bridges and structures are examples.

Research towards the effect of corrosion of the steel reinforcement on the load carrying capacity of Reinforced Concrete (RC) beams have been well reported (Mangat and Elgarf, 1999; Cabrera, 1996; Rodriguez *et al.*, 1997; Castel *et al.*, 2000a, b; Coronelli and Gambarova, 2004). However, most corroded RC beams investigated still have their reinforcement and concrete work together with reduction of the bond strength. There is little research on the severely corroded RC beams. The severely corroded RC beams investigated in this study have more than 1/3 part of main reinforcement lost bond with concrete due to spalling of concrete cover. The behaviour of those

severely corroded RC beams may have significant difference from those uncorroded RC beams. The deteriorate degree of reinforcing concrete members in a structures usually are different due to different locations, loading and so on. Those members having heavy deterioration are the weak points of the whole structures. Therefore, it is important to know the behaviour of those beams.

It can be quite costly and time consuming for experimental investigation, therefore, numerical method has been used to investigate the behaviour of corroded RC members (Coronelli and Gambarova, 2004; Dekoster *et al.*, 2003). This study was conducted in Zhejiang university in 2010. In this study, the finite element program ABAQUS (2004) is used to simulate RC beams with heavy deterioration. The purpose of the study is to investigate the behaviour of severely corroded RC beams through experimental investigation and numerical simulation. Parametric study was also conducted to investigate the effect of different parameters on the residual strengths of corroded RC beams.

MATERIALS AND METHODS

Test program:

- General: Three naturally corroded RC beams with nominal dimensions of L = 6000 mm, h = 800 mm

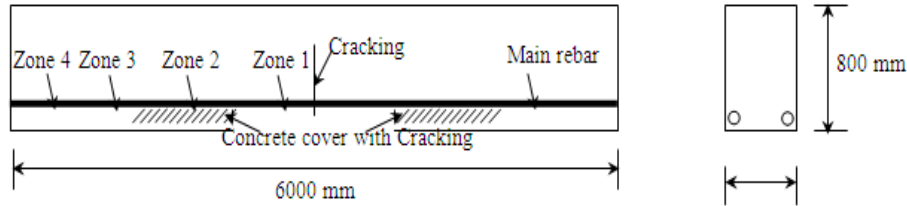


Fig. 1: Test RC beams heavy deterioration

Table 1: Corrosion rate of rebar obtained from different locations

Location	Zone 1	Zone 2	Zone 3	Zone 4
Corrosion rate ψ (%)	63.3	45.2	18.1	0.0

Table 2: Corrosion rate of rebar obtained from different locations

Location	Zone 1				Zone 2		
ψ (%)	57.2	57.8	40.2	39.8	30.6		
Tensile strength (kN)	40.5	43.5	82.0	83.0	120.0		
Location	Zone 3				Zone 4		
ψ (%)	12.6	13.9	19.4	23.2	4.0	4.0	0.0
Tensile strength (kN)	102.0	112.0	107.0	126.5	103.0	167.0	183.0

and $b = 400$ mm were investigated. The three corroded RC beams were taken from a coastal dock built in 1980. Dimensions and reinforcement details of the corroded RC beams tested were shown in Fig. 1. The design grade of concrete is C30 and the depth of concrete cover is 25 mm. The nominal diameter of longitudinal rebar was 20 mm with nominal yielding strength of 335 MPa and ultimate strength of 490 MPa. A careful inspection was done for the tests beams before the loading tests. Deterioration of beams such as crackling of concrete cover, loss of concrete cover was recorded. Details were presented in Chen (2002).

Material tests: Concrete cylinder and corroded rebar for material tests were taken from the extra specimen obtained from the same dock. Concrete cylinder having diameter of 100 mm and length of 150 mm were tested for compression strength. The average compression strength (f_c) for 9 concrete cylinder specimens are 33.1 MPa. The corrosion rate of reinforcement in the different part of corroded beams were firstly measured. Rebar having length of 100 mm was taken from four zones of the beams as shown in Fig. 1. The rebar was retrieved from the concrete and the corrosion products cleaned employing a corrosion-inhibited HCl solution (Bertoa *et al.*, 2008). The mass loss of the steel rebar (W_G) was estimated afterwards by subtracting the post-corrosion mass from the nominal pre-corrosion masses. The corrosion rate (ψ) for the rebar were calculated as: $\psi = (W_G - W_G)/W_G\%$. The estimated values of ψ for rebar obtained from different locations are

presented in Table 1. Tensile tests were also carried out on the rebar having different corrosion rate. The test results were presented in Table 2. Generally, the tensile strength of corroded rebar decreases with the increase of corrosion rate.

Beam tests: The beams were loaded in the mid-span with the two ends simply supported, as shown in Fig. 2. LVDT was used to measure the mid-span deflection of the beams. In addition, 12 linear strain gauges were used to measure the strain of rebar and concrete of each tested beam. A load interval of approximate 4 kN was used. Each load interval was maintained for about 2 to 3 min. At each load increment the strain readings and the mid-span deflection were recorded. A load interval of approximate 1 kN was used near failure. All specimens were loaded to failure. Each test took approximately 1 hour to complete.

The failure mode of those severely corroded RC beams was different from those uncorroded beams. The cracking in the midspan increasing with the increasing loading. The concrete cover in the mid-span delaminate from the beams with the increase of load. At the point of ultimate load, the concrete in compression crushed. Finally, the longitudinal rebar was broken. The ultimate loads for three tested beams A, B and C were 23, 24 and 24 kN, respectively. The midspan deflection versus load curves of tested beams were also plotted, as shown in

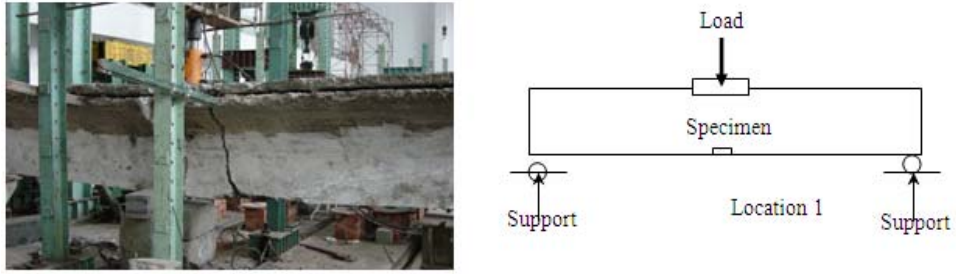


Fig. 2: Loading test of corroded RC beams

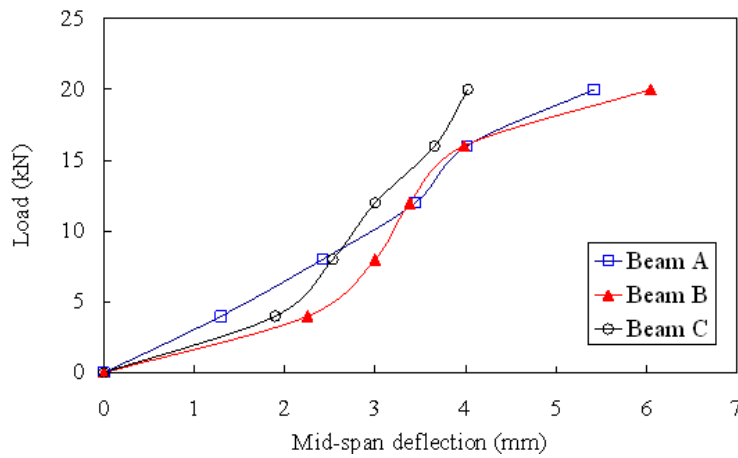


Fig. 3: Mid-span deflection versus load curves of tested specimens

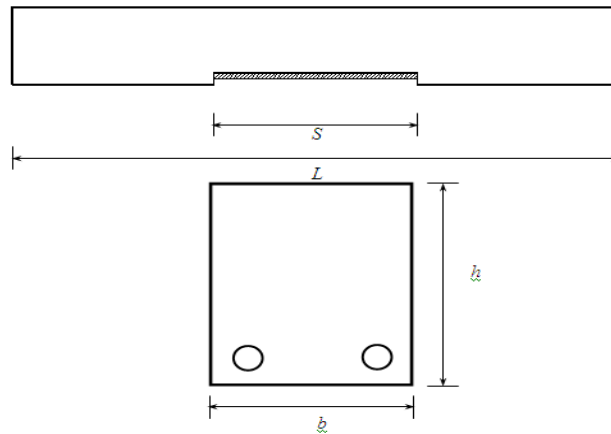


Fig. 4: Definition of symbols

Fig. 3. Since the LVDT was remove before the failure of the beams, the load-deflection curves is plotted up to 20 kN. The reading of strain gauge on the concrete at the middle span of the beam just above the rebar (Location 1) indicates that the tensile stress in the concrete could be

negligible. The reading of strain gauge at the same location but on the rebar below the indicates that the tensile stress in the rebar under the loading of 20 kN was approximate 160 MPa which is far tensile stress of corroded rebar obtained from the material tests above.

Therefore, it may be concluded that the failure of the beams was the crush of the concrete in the compression zone.

Design: The design strength of the uncorroded RC beams having the same dimensions and rebar could be calculated using the design value of material properties as below:

$$\begin{aligned} \sum x &= 0, f_c b x = f_y A_s \\ \sum M &= 0, M = f_y A_s (h_0 - x/2) \end{aligned} \quad (1)(2)$$

where, A_s is the cross-section area of rebar; b is the width of the beam; f_c is the concrete design compressive strength, f_y is the yielding strength of rebar; h_0 is the distance from the rebar to the top surface of the beam; and x is the height of the compressive zone of the concrete.

The design strength of the uncorroded beams are 157.6 kN.m which was more than four times of the test results of the corroded beams (average strength of three tested beams = 35.4 kN.m). It may be explained by the deterioration of the material properties, especially the rebar. Therefore, the residual strength of corroded beams was also calculated using Eq. (1) and (2) by substituting the material properties obtained from the material tests. The tensile strength of rebar (f_{y_s}) was taken as the minimum value in Table 2 = 40.5 kN. The concrete compressive strength was taken as 80% of the cylinder tests results (26.5 MPa). Thus the design strength of corroded beams was 61.5 kN.m, which was still almost twice of the test results of the corroded beams.

From the comparison above, it could be seen that the design method using Eq. (1) and (2) are very unconservative and seems not applicable for severely corroded beams tested in this study. However, due to the limitation of the test data, further investigation was necessary to study the behaviour of RC beams with heavy deterioration. Therefore, finite element method was used in this study.

Finite element model and verification: The finite element program ABAQUS (2004) was used in the analysis of RC beams with heavy deterioration in this study. Since the concrete cover spalling and corrosion of longitudinal rebar were mainly concerned in this study, the stirrups was not considered in the finite element model. In the finite element model, the reinforcing bars were modeled as rebar layer, as specified in ABAQUS manual (2004). The effect of concrete cover spalling on the bond between the concrete and rebar was simulated by introducing the dependence on the state of the surrounding concrete (Bertoa *et al.*, 2008). In this study, the concrete and rebar was considered as almost have no bond in the concrete cover spalling zone. Therefore, the concrete surround the rebar was modeled to have 1%

material properties (elastic modulus, yield strength and ultimate strength) of normal concrete in the finite element model.

Finite element type and mesh: The four-node bilinear plain stress element CPS4 was used in the model. The element has two degree of freedom per node. In order to choose the finite element mesh that provides accurate results with minimum computational time, convergence studies were conducted. The main part of the concrete has a 20 mm × 20 mm (length by height) ratio. It is found that such a mesh provides adequate accuracy in modeling the RC beams with minimum computational time.

Boundary conditions and load application: The RC beams were modeled as simply supported at two ends and loaded in the mid-span, as shown in Fig. 4. The bearing plates at both ends of the beams and the loading plate were modeled using kinematic coupling constraints. In general, a kinematic coupling constraints is used to impose constraints between degrees of freedom of a node set and the rigid body motion defined by a reference node. It should be noted that only the degrees of freedom specified were constrained. For example, only the y direction degree of freedom of the loading part of the beam is constraint since the loading plate apply a y direction displacement on the beams. The x direction displacement of the loading part was not constrained. Since the constrained degrees of freedom of cinematic coupling constrained nodes can be prescribed by applying boundary conditions at the rigid body reference node, the restraints were applied on the reference point in this study. The reference point at the loaded part was restrained against x directions but free to move against y -axes. The reference point at the support ends were restrained against x and y directions.

The load was applied in increments using the modified RIKS method available in the ABAQUS library. The RIKS method is generally used to predicted unstable and nonlinear collapse of a structure. It uses the load magnitude as an additional unknown and solves simultaneously for loads and displacements. Since considerable nonlinearity is expected in the response of this model, including the possibility of unstable regimes as the concrete cracks, the modified RIKS method is used with automatic incrementation in the analysis. The nonlinear geometry parameter (NLGEOM) was included to deal with the large displacement analysis. The load was applied at the reference point of the loaded part by specifying a certain displacement. Since the concrete cracking must be considered in the analysis, the parameter ANALYSIS = DISCONTINUOUS is included in the option of CONTROLS.

Table 3: Comparison of FEA results with experimental results

Specimen	TES $M_{u,TEST}$ (kN.m)	TFEA $M_{u,FEA}$ (kN.m)	Comparison $M_{u,TEST}/M_{u,FEA}$
Beam A	23	22	1.05
Beam B	24	22	1.09
Beam C	24	22	1.09

Material model: The material properties of concrete and corroded rebar are taken from material tests. Some of those data are assumed values, because they are not available for the concrete used in the experiment. The assumed values are taken from typical concrete data. The modeling of the concrete the concrete-reinforcement interaction and the energy release at cracking is of critical importance to the response of a structure such as the concrete starts to crack. ABAQUS (2004) modeled those effects in a direct way by adding tension stiffening to the plain concrete model. The simplest tension stiffening model defines a linear loss of strength beyond the cracking failure of concrete. In this study, the critical displacement beyond failure at which all strength is lost (0.05 mm) are used to illustrate the effect of the tension stiffening parameters on the Responses. Since the response of the beams is dominated by bending, it is controlled by the material behavior normal to the crack plans. The material shear behaviour in the plane of crack is not important. Consequently, the choice of shear retention has no significant influence on the results. The elastic-plastic material model of bar is adopted in this study.

Verification: The corroded tested was modeled in this study. The loss of concrete cover and initial crack was modeled. The ultimate strength obtained from the numerical analysis was compared with test results in Table 3. It is shown that the numerical results reasonably agree with the test results well. The maximum difference between the numerical and experimental results is 9%.

RESULTS AND DISCUSSION

It is shown that the finite element model developed in this study could predict the residual strength of corroded beams with reasonable accuracy. Therefore, parametric study was carried out using finite element model. A beams having small size of (L = 1600 mm, h = 200 mm, b = 200 mm) was modeled for computational time and avoid convergence problem, as shown in Fig. 5. Two longitudinal rebar having diameter of 20 mm were used with depth of concrete cover of 25 mm. The yielding strength (f_y) of the re bar was 235. The concrete material properties is taken from Gilbert and Warner (1978) shown in Table 4. Parametric study was conducted to investigate the effect of different length of concrete cover spalling and loss of rebar cross-section area on the behaviour of corroded beams. The specimens were labeled that the length of concrete cover spalling and reduction factor of rebar cross-section area could be identified from the labels. The first letter is spalling of concrete cover,

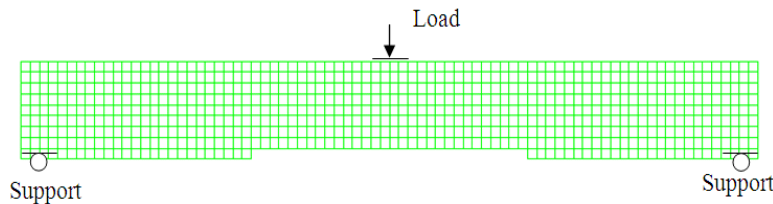


Fig. 5: Finite element model

Table 4: Concrete material properties used in the parametric study [13]

Elastic modulus E (Gpa)	28.6
Poisson's ratio ν	0.15
Yield stress f_{cy} (Mpa)	20.68
Failure stress f_{cu} (Mpa)	37.92
Plastic strain at failure ϵ_u	1.5×10^{-3}
Ratio of uniaxial tension to compression failure stress	8.6×10^{-2}
Ratio of biaxial to uniaxial compression failure stress	1.16
Cracking failure stress (Mpa)	3.17

Table 5: Reduction factor of specimen bending strengths

Specimen	Length of concrete cover spalling (mm)	Reduction factor of rebar area	Reduction factor of bending strength
S00R100	0	1.00	1.00
S120R90	120	0.90	0.90
S200R80	200	0.80	0.80
S280R70	280	0.70	0.72
S360R60	360	0.60	0.63
S480R50	480	0.50	0.55
S600R40	600	0.40	0.48

followed by the length of mm. The letter refer to the reduction factor of cross-section area, followed by value of factor in percentage. For example, the specimen 120R90 was specimen having concrete cover spalling length of 120 mm with reduction factor of rebar cross-section area of 90%.

The mid-deflection versus load curves of specimens having different length of concrete cover spalling was plotted in Fig. 6. It is shown that the different length of concrete cover spalling almost has no effect on the bending strengths of RC beams. However, the rigidity of the beams decreases with the increase of concrete cover spalling lengths. The ultimate strengths of beams having different length of concrete cover spalling and loss of rebar cross-section area were presented in Table 5. The mid-deflection versus load curves were plotted in Fig. 7. It is shown that the ultimate strengths decreases with the increase of rebar cross-section area loss. It could be seen that the reduction factors of specimen strength were generally similar with the reduction factor of loss of rebar cross-section area. The comparison also indicates that the reduction factor of bending strength is gradually larger than the reduction factor of rebar cross-section when the corrosion rate increases.

The design strengths obtained from Eq. (1) and (2) for specimens from S000R100 to S600R40 were compared with the FEA results in Table 6. It is shown that

the design strengths predicted by Eq. (1) and (2) were conservative. The comparison ratio ($M_{u,FEA}/M_{u,design}$) decreases with the increases of reduction factors of rebar cross-section area. It is also shown that the reduction factor of specimen strengths become larger than the reduction factor of rebar cross-section area with the increase of corrosion rate. The reason may be that the tensile strength of concrete is neglected in the design. However, the effect of tensile strength of concrete increases with the decrease of rebar cross-section area in the FE analysis. The vertical crack at the mid-span of beams was observed from the two of three tested specimens. Therefore, the effect of vertical crack at the mid-span of beams was also investigated. The parametric study was carried out on specimen S600R40, since there may be no vertical crack for beams without heavy deterioration. The lengths of vertical crack for specimen S600R40-C60, S600R40-C100, and S600R40-C140 were 60, 100 and 140 mm, respectively. The mid-span deflection versus load curves were plotted in Fig. 8. It is shown that the mid-span vertical crack has effect on the rigidity and strengths of corroded beams. It is also shown that the specimen ultimate strengths decreases with the increase of the vertical crack length. The maximum reduction factor of specimen ultimate strengths due to vertical crack was 81.7% (Table 7).

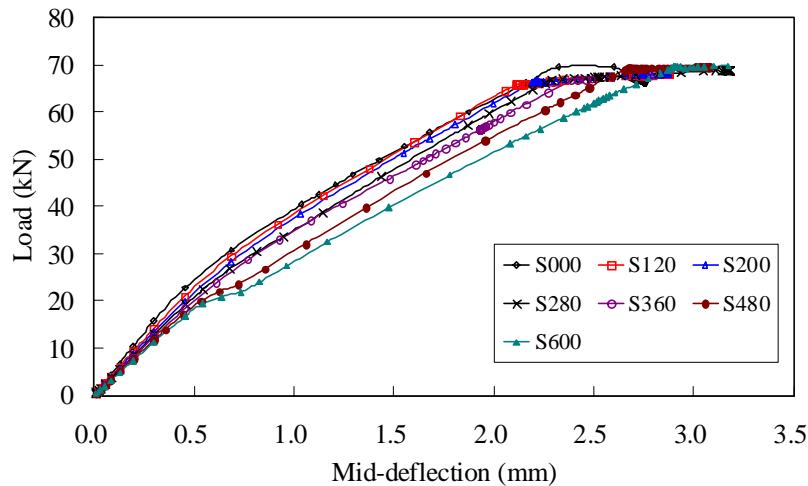


Fig. 6: Deflction-load curves for specimens having different length of concrete cover spalling

Table 6: Comparison of design strengths with FEA results

Specimen	FEA $M_{u,FEA}$ (kN.m)	Design $M_{u,design}$ (kN.m)	Comparison $M_{u,FEA} / M_{u,design}$
S000R100	27.8	23.7	1.17
S120R90	25.9	21.4	1.21
S200R80	23.6	19.2	1.23
S280R70	22.4	16.9	1.33
S360R60	19.6	14.5	1.35
S480R50	17.1	12.2	1.40
S600R40	15.0	9.8	1.53

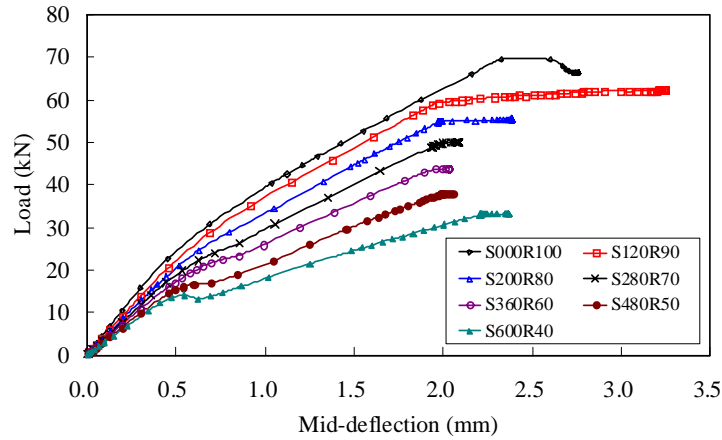


Fig. 7: Deflection-load curves for specimens having different length of concrete cover spalling and rebar cross-section reduction

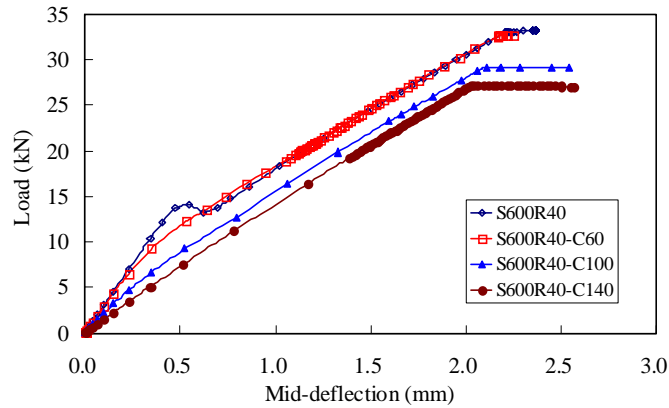


Fig. 8: Deflection-load curves for specimen S600R40 with different length of mid-span vertical crack

Table 7: Bending strength of specimen S600R40 with different lengths of mid-span crack

Specimen	Ultimate strength	
	$M_{u,FEA}$ (kN.m)	Reduction factor
S600R40	33.26	1.00
S600R40-C60	32.67	0.98
S600R40-C100	29.22	0.88
S600R40-C140	27.19	0.82

However, if the vertical crack penetrates the beam from the bottom to the top, the reduction factor of specimen ultimate strength is dramatically lower (20%). This may be the possible reason for the low strength of tested specimens. It is also observed from the tests that the concrete crushed before the broken of longitudinal rebar. Since strength calculated using Eq. (1) and (2) are based on the failure of rebar, it was different from the failure of test specimens.

CONCLUSION

Experimental and numerical investigation of RC beams with heavy deterioration were conducted in this

study. Three naturally corroded RC beams were investigated. Both material tests and beam bending tests were carried out. Test result obtained from the loading tests were compared with design strength by substituting the damaged material properties. It is shown that the design strength was unconservative. Finite element method was used to further investigate the behaviour of RC with heavy deterioration. The effect of concrete cover spalling, loss of rebar cross-section area and mid-span vertical crack were studied through parametric study. It is shown that the length of concrete cover spalling has negligible effect on the strengths of corroded RC beams but has the effect on the rigidity. It is also shown that strength of corroded RC beams decrease when the loss of rebar cross-section increases. The design strengths are conservative for corroded beams with concrete cover spalling and loss of rebar cross-section area. The specimen ultimate strengths decreases with the increase of the vertical crack length. The vertical crack penetrate the specimen may be the reason of the low strength of tested specimens.

ACKNOWLEDGMENT

The research of this study is supported by Shenzhen Key Lab on Durability of Civil Engineering (SZDCCE11-01).

REFERENCES

- ABAQUS, 2004. ABAQUS analysis user manual. Version 6.5. ABAQUS, Inc.
- Andrs, A.T, N. Sergio and T. Jorge, 2007. Residual flexure capacity of corroded reinforced concrete beams. *Eng. Struct.*, 29(6): 1145-1152.
- Bertoa, L., B. Simionib and B. Saettab, 2008 Numerical modelling of bond behaviour in RC structures affected by reinforcement corrosion. *Eng. Struct.*, 30(7): 1375-1385.
- Cabrera, J.G., 1996. Deterioration of concrete due to reinforcement steel corrosion. *Cement Concrete Composit.*, 18(1): 47-59.
- Castel, A., R. Francois and G. Arliguie, 2000a. Mechanical behaviour of corroded reinforced concrete beams-Part 1: Experimental study of corroded beams. *Mater. Struct.*, 33(5): 39-44.
- Castel, A., R. Francois and G. Arliguie, 2000b. Mechanical behaviour of corroded reinforced concrete beams-Part 2: Bond and notch effects. *Mater. Struct.*, 33(5): 45-51.
- Chen, J., 2002. Study on durability of reinforced concrete members due to chloride ingress. M.Phil Thesis, Zhejiang University.
- Coronelli, D. and P. Gambarova, 2004. Structural assessment of corroded reinforced concrete beams: Modeling guidelines. *J. Struct. Eng. ASCE*. 130(8): 1214-24.
- Dekoster, M., F. Buyle-Bodin, O. Maurel and Y. Delmas, 2003. Modelling of the flexural behaviour of RC beams subjected to localised and uniform corrosion. *Eng. Struct.*, 25(10): 1333-41.
- Gilbert, R.I. and R.F. Warner, 1978. Tension Stiffening in Reinforced Concrete Slabs. *J. Struct. Division, ASCE*. 104(12): 1885-1900.
- Pandey, J. L. and M.K. Banerjee, 1998. Concrete corrosion and control practices-An overview. *Anti-Corros. Methods Mater.*, 45(1): 5-15.
- Rodriguez, J., L.M. Ortega and J. Casal, 1997. Load carrying capacity of concrete structures with corroded reinforcement. *Constr. Build. Mater.*, 11(4): 239-248.